PREDICTING SHADING LOSSES IN PHOTOVOLTAIC PLANTS: A NOVEL APPROACH

D. López Dalmau[1], H. Mirandona López[1], C. Javier Lopes Gomes[1], J. Tomàs Villalonga Palou[1], C. Rossa[1]
[1]Sunveon
calle del Musgo, 2, 1B, Madrid, Spain. 28023

ABSTRACT: Accurately estimating shadow impact on large-scale photovoltaic (PV) plants is challenging due to the computational demands of traditional methods. This study introduces the Sunveon Model, a novel, efficient approach for simulating shading and mismatch losses without requiring complex I-V curve calculations. The model uses a hybrid methodology, combining a 2D irradiance model with a 3D submodule-level shading model. Its key innovation is the use of a regression model, whose accuracy was validated against over 500,000 I-V curves, to directly predict a string's Maximum Power Point (MPP), significantly reducing computational time. It also quantifies mismatch losses with a new 'Mixed Fill Factor' that establishes a direct quadratic relationship between losses, shadow percentage, and irradiance. Validated against real-world data, the Sunveon Model proved more accurate than two industry-standard models, showing substantially lower errors. A key finding is that mismatch losses for standard cells are about 64% higher than for half-cell modules. In summary, the Sunveon Model offers a precise and efficient tool for large-scale PV analysis.

Keywords: Shading-induced losses, mismatch losses, computational efficiency, 3D shading model

1 INTRODUCTION

Accurately estimating the impact of shadows on photovoltaic generation is significantly constrained by the current scale of photovoltaic (PV) plants and the complexity of the terrain. This challenge is compounded by the excessive computational cost associated with calculating complete I-V curves, which restricts their application in precisely estimating energy production from large-scale PV plants. For example, on a conventional PC, a typical 50 MW plant (about 3,000 strings) can be simulated in 30 seconds for shading table generation (12×13 positions per string) plus 50 seconds for yield simulation. This has motivated most standard production models available on the market to simplify yield estimations, working with statistical approaches to simulate the impact of shadows on current PV plants[1], [2], [3], which can be hundreds of megawatts in size. These models typically simulate only a few representative strings within the plant, leading to over or underestimating shading effects due to common loss factors. This, in turn, affects accurate assessment of mismatch losses.

This study proposes a novel approach to simulate shading-induced losses in PV plants without the need to compute complete I-V curves, thereby significantly reducing computational costs. Additionally, it proposes a method to estimate the mismatch losses due to different shade patterns throughout the strings.

2 METHODOLOGY

2.1 How the Sunveon Model works

Using a dataset of over 500,000 I-V curves from different manufacturers and spanning various shading and irradiance conditions, we developed linear regressions to accurately predict losses for standard and half-cell modules. This approach eliminates the need to calculate new I-V curves for every simulation, capturing the electrical effects in all possible shading scenarios in an actual PV plant. The impact of series and shunt resistances was very low in all cases and could be considered negligible.

From one of the classical transposition models[4], [5], the model uses a distinct approach to more precisely estimate diffuse and reflected irradiance on both the front and rear sides of modules. It estimates the shading effects on diffuse irradiance caused by surrounding structures, considering the shading state of the terrain[6], [7]. To achieve that, the model follows these steps:

1. The process begins by defining the basic parameters of a 2D scenario (Fig.1). This includes the characteristics of the structure (e.g., type, dimensions, axis height, pitch between rows, transparency, module spacing, number of modules, width, bifaciality), terrain characteristics (slope, albedo), and the location's latitude. The scenario sets the positions of the axes of five simulated rows of structures (either fixed-tilt or tracking). A constant slope is set for these five rows, as well as the terrain limits, and their normal and directional vectors. Latitude is important as it influences the sign of the slope angle, especially for fixed structures.
2. Since the scenario's composition is affected by the sun's position (structure rotation, projected shadows), some of its geometry must be recalculated at each interval. This involves calculating the solar ray vector in the 2D scenario by transforming its coordinates from a global reference system to the local 2D system. The position of the collectors and their segments are then calculated, attributing an index to each. For fixed structures, segment positions are constant, but for trackers, positions are calculated based on structure rotation, which depends on sun position and tracking strategy. The model also determines if segments are shaded or not.
3. Once segment locations and indices are calculated, view factors between them are determined. This involves calculating factors towards adjacent row segments, ground segments, and finally, the sky. Reciprocity is

10.4229/EUPVSEC2025/4DV.4.3
020432-001

used to avoid unnecessary calculations. Obstructions between segments are also accounted for when calculating lengths and diagonals.

4. Possible incident irradiance values are calculated for each segment type (front, back, ground) and shading scenario (illuminated/shaded), breaking it down into direct, circumsolar diffuse, and horizontal diffuse components. Isotropic diffuse component is treated differently, with its value inherently incorporating shadow effects, eliminating the need to differentiate between shaded and illuminated states. The model calculates direct irradiance for each segment type, considering the solar ray's incidence angles. The classical transposition methods[4], [5] are then applied, by removing the effect of coefficients dependent on inclination or incidence angle (Fig.2).
5. The model combines a 2D irradiance model with a 3D shadow calculation model. The 2D model discretises surfaces like structures and the ground into segments to calculate irradiance exchange using view factors. It provides the incident irradiance for two states: illuminated and shaded. These results are then combined with the 3D model, which provides information on the number of shaded submodules within a string. This new approach streamlines the process by focusing on the binary illumination states and the specific proportion of shaded submodules (Fig.3 and Fig.4).

Following these steps, the incident irradiance on both the front and rear of the central simulated row is estimated under illumination and shading conditions. This calculation, which is assumed to be the valid result, provides a detailed characterisation of incident irradiance in partially shaded rows. This results in a characteristic incident irradiance for each binary state of the submodules, either shaded (active bypass diode) or illuminated (no active bypass diode)[8], resulting in a characteristic I-V curve for the array formed by half-cell (Fig.5) or standard (Fig.6) modules. The output of the 2D irradiance model is then combined with a 3D submodule-level shading model, where individual strings exhibit different shadow patterns, and consequently, varying proportions of affected submodules. This analysis accounts for two key factors related to shading. First, the shading state is not a total absence of light; it specifically includes the amount of diffuse irradiance reaching shaded cells. Second, we consider edge effects, such as the minimum shadow cast by the module's frame, which would affect the entire submodule.

The Fig 1. depicts the 2D scenario defined by the model in the step 1. As a representative case of the model, the Fig. 2 depicts the global irradiation along a sunny day obtained from the Perez transposition model (grey line), and for both illuminated and shaded parts of the string calculated by the Sunveon model (blue and orange lines). Fig. 3 and Fig. 4 depict two 3D scenarios with their corresponding shading factor (% of shaded submodules) at each string of a PV Layout. The Fig. 5 and Fig. 6 depict, respectively, an I-V curve used to obtain the regression models from half-cell and standard modules.

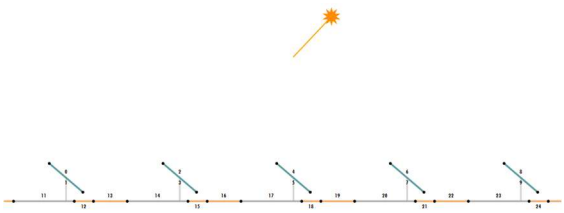

Figure 1: 2D scenario defined by the model

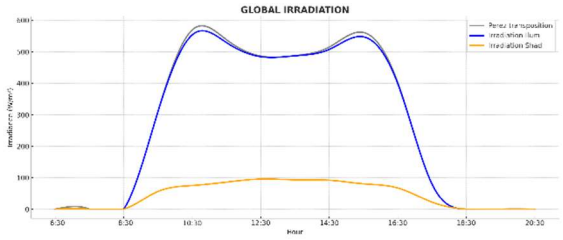

Figure 2: Global irradiation for illuminated and shades parts of a string, obtained from the Perez transposition model

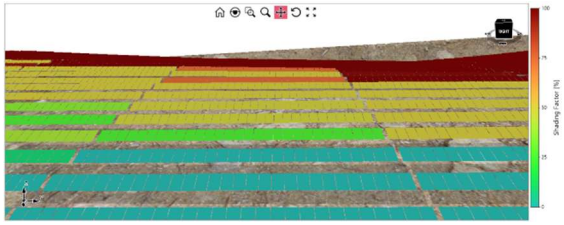

Figure 3: 3D scenario depicting a front view of a PV plant illustrating the distribution of the shading factor. The darker the string's colour, the more shaded it is relative to the most illuminated string

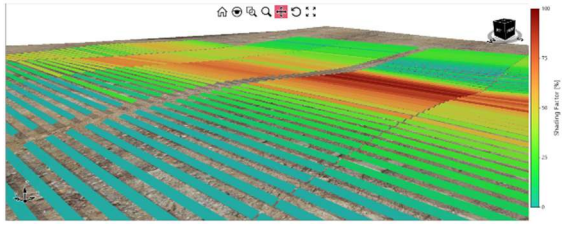

Figure 4: 3D scenario depicting a diagonal view of a PV plant illustrating the distribution of the shading factor. The darker the string's colour, the more shaded it is relative to the most illuminated string

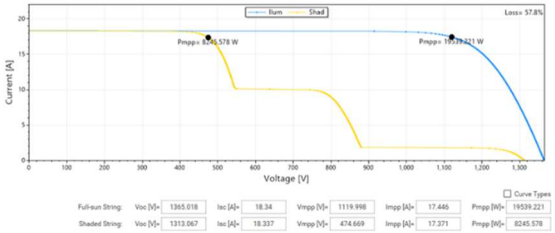

Figure 5: I-V curve of an illuminated and a shaded string of half-cell PV modules

10.4229/EUPVSEC2025/4DV.4.3
020432-002

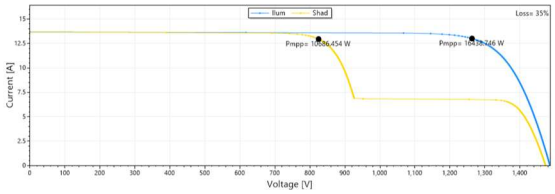

Figure 6: I-V curve of an illuminated and a shaded string of standard PV modules

The Sunveon Model is applicable to both standard and half-cell modules. It combines irradiance and shading models to estimate the Maximum Power Point (MPP) of each individual string within a solar plant, taking into account the mismatch losses induced by shadows. Unlike traditional methods, it doesn't require a full I-V curve calculation for every string. Instead, the regressions obtained from the over half a million I-V curves provide the necessary parameters to accurately estimate the energy production. We can extend the estimations to an entire PV plant by a precise calculation of input conditions for inverter MPPTs, allowing a granular production within any layout (Fig.7).

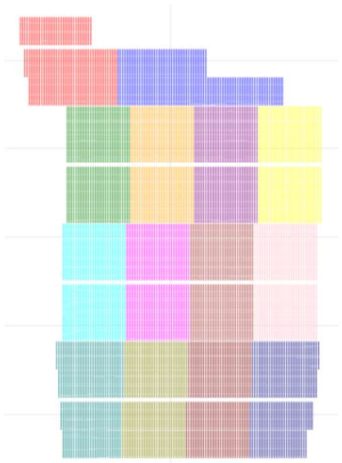

Figure 7: Electrical Layout (Power blocks) of a 70 MW_p plant

It is worth commenting that the model in its complete version also includes other types of losses, such as IAM, soiling and thermal losses induced by the wind[9], but their detailed description is beyond the scope of this article. Here we opted to make a description only for the ways to obtain a more precise irradiance reaching the modules. In this case, here we consider the intrinsic mismatch losses between the modules as null[10], [11].

3 RESULTS AND DISCUSSION

3.1 Benchmark validation

The model was validated against over 500,000 I-V curves, which resulted from shading patterns observed in real PV layouts (from five different PV plants, ranging from approximately 5 to 150 MW_p) under diverse incident irradiance conditions. The same analysis was also conducted using two other shadow models often used in the industry. The I-V curves derived from these various shading patterns are considered the 'real losses,' and the performance of all three models (the two industry-standard models and the Sunveon Model) is plotted against these real losses for comparison.

The models are described below:

- Model 1: it reduces the beam component of the incident irradiance according to percentage of shaded submodules, then it computes the MPP power (P_{MPP}) of the string (single-diode model)[12], [13].
- Model 2: it computes the P_{MPP} at illumination and shade conditions, then computes a new value that lies in-between both, depending on the shading factor[14].
- Sunveon Model: it uses a novel regression model with the following inputs: P_{MPP} at illumination, proportion of shaded submodules in the string and proportion of incident diffuse irradiance. A specific model is developed both for standard and half-cell modules.

3.2 The reliability of the Sunveon Model

As a representative case, Fig. 8 and Fig. 9 summarise the comparison between simulated I-V curves of a single string under various shading patterns and irradiance conditions. The results from the Sunveon Model (yellow squares) are presented alongside those from two industry-standard models, Model 1 (red diamonds) and Model 2 (blue triangles), for both standard and half-cell modules. The findings from large-scale numerical tests are detailed in Table I (Standard modules) and Table II (Half-cell modules), located below their respective figures.

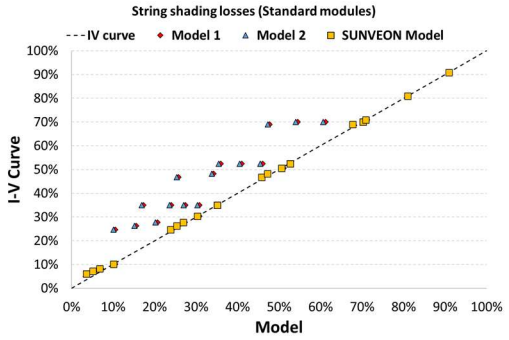

Figure 8: I-V Curve vs Shading loss models for Standard modules

Table I: Large-scale numerical testing (Standard modules)

	MAE [%]	STD [%]
Model 1	4.26	5.49
Model 2	6.48	4.76
Sunveon Model	0.79	1.53

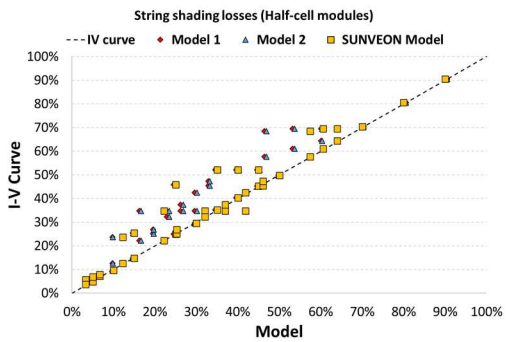

Figure 9: I-V Curve vs Shading loss models for Half-cell modules

10.4229/EUPVSEC2025/4DV.4.3
020432-003

Table II: Large-scale numerical testing (Half-cell modules)

	MAE [%]	STD [%]
Model 1	7.05	5.61
Model 2	6.99	5.62
Sunveon Model	1.36	2.28

The results from both Standard and Half-cell modules consistently demonstrate the superior accuracy and reliability of the Sunveon Model compared to Model 1 and Model 2, reflected both in their Mean Absolute Error (MAE) and Standard Deviation (STD). In both cases, the Sunveon Model aligns remarkably closely with the benchmark (the real I-V curve data), while the other models consistently underestimate losses, with their predictions typically falling above the diagonal when plotted against actual values. The following comments apply:

For Standard Modules:

- The Sunveon Model exhibits remarkably low error rates with an MAE of 0.79% and an STD of 1.53%. This precision is evident in its close alignment with the benchmark.
- Model 1 shows significantly higher errors with an MAE of 4.26% and an STD of 5.49%.
- Model 2 also presents elevated errors, with an MAE of 6.48% and an STD of 4.76%.

For standard modules, the Sunveon Model greatly outperforms the other models, with its MAE being approximately 5 to 8 times lower than that of the other two models and its STD approximately 3 times lower, indicating a far more precise and consistent prediction capability.

For Half-cell Modules:

- The Sunveon Model continues to show strong performance, with a MAE of 1.36% and a STD of 2.28%. While slightly higher than for standard modules, these values remain exceptionally low, confirming the model's robustness.
- Model 1 presents an MAE of 7.05% and an STD of 5.61%.
- Model 2 shows similar performance to Model 1, with an MAE of 6.99% and an STD of 5.62%.

A similar trend is observed in half-cell modules; though the Sunveon Model's errors are slightly higher (MAE 1.36%, deviation 2.28%), this is expected due to the more complex electrical topology of half-cell modules, consisting of six submodules arranged as two parallel strings of three submodules in series. Despite this, the estimation remains highly precise. Even in this more challenging scenario, the Sunveon Model maintains a substantially lower MAE (approximately 5 times lower) and STD (about 2.5 times lower) compared to Model 1 and Model 2. The trend of Model 1 and Model 2 consistently underestimating losses persists, albeit with some points deviating further from the diagonal, indicating less precision than for standard modules.

3.3 Mismatch losses due to different shading patterns

Each string, with its respective illumination and/or shading pattern, has a unique electrical characteristic and, consequently, an associated Fill Factor (FF). The parallel connection between these strings subsequently leads to instantaneous mismatch losses[15]. Based on the Sunveon Model, we were able to derive a new mismatch loss model that is applicable for estimating these losses in parallel strings due to different shading patterns. We describe this model below, step by step:

- Firstly, it is established a unique series of n modules, and then, 10 random different shading patterns (from about 0.5% to about 90%) are applied for each irradiance value, ranging from 100 W/m² to 900 W/m², in increments of 50 W/m².
- Each of these simulation conditions (shade and irradiance) generates an electrical response, and consequently, an individual FF. To assign an appropriate weight to both illuminated and shaded areas, we considered the FF here as the ratio between the maximum power in shade and the product of V_{oc} and I_{sc} in illumination. To differentiate this from the original concept of FF, we have termed this relation the 'Mixed Fill Factor,' calculated as:

$$FF_{mix} = \frac{I_{\mathrm{MPP,shd}}\, V_{\mathrm{MPP,shd}}}{I_{\mathrm{sc,illum}}\, V_{\mathrm{oc,illum}}} \quad (1)$$

  where $I_{\mathrm{MPP,shd}}$ and $V_{\mathrm{MPP,shd}}$ are the current and voltage at the maximum power point in shading conditions and $I_{\mathrm{sc,illum}}$ and $V_{\mathrm{oc,illum}}$ are the short-circuit current and open-circuit voltage in illumination. It is worth commenting that the error in using the values in illumination rather than in shading conditions is no more than 3% in the worst cases.
- For each irradiance value, there are 10 different FF_{mix} values. The coefficient of variation of these values can now be calculated by the relation between the associated standard deviation and the mean value (Equation 2):

$$CV_{FF,mix} = \frac{\sigma_{FF_{mix}}}{\overline{FF_{mix}}} \quad (2)$$

- The ten strings combined in a single MPPT give rise to a characteristic I-V curve with its respective electrical patterns due to the different shades in each string. The ratio between the total power of this hypothetical shaded array and the sum of the individual power of each shaded string give rise to an electrical mismatch loss, i.e.:

$$EMM_{shd}(\%) = 1 - \frac{P_{total,array,shd}}{\sum_1^n P_{i,n\,string,shd}} \quad (3)$$

- A relationship between $EMM_{shd}(\%)$ and

10.4229/EUPVSEC2025/4DV.4.3
020432-004

$CV_{FF,mix}$ is then established (R^2>0.95). Equation 4 allows to calculate the mismatch losses directly from the method described in section 2.1 – i.e. for parallel connections-, now without the need to calculate any I-V curve. The relationship is also seen in Fig. 10.

$$EMM_{shd}(\%) = 0.0076\ CV_{FF,mix}(\%)^2 + 0.2445\ CV_{FF,mix}(\%) \quad (4)$$

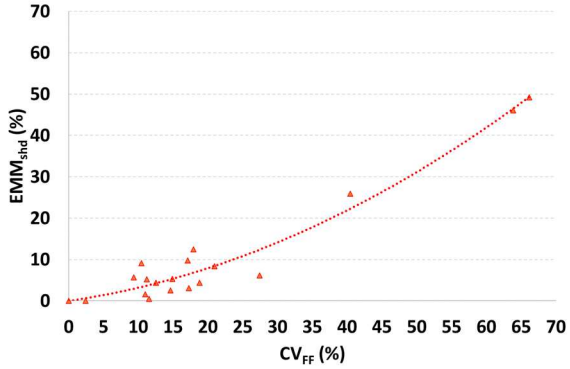

Figure 10: Relationship between the percentual values of Electrical Mismatch Losses (EMM_{shd}) and coefficient of variation of Mixed Fill Factor ($CV_{FF,mix}$)

Previous studies have also established a quadratic relationship for mismatch losses[11], [16], [17], [18], though mainly focused on series connections.

3.4 Mismatch losses for standard and half-cell modules

Mismatch losses between strings vary significantly depending on the shading conditions across different strings and also on the irradiance in the illuminated sections. One can intuitively infer that higher irradiances lead to greater mismatch losses, as the illumination gradient between shaded and illuminated areas becomes more pronounced. However, the precise magnitude of these losses is the key question. Equation 6 allows us to shed some light on these questions. Fig. 11 shows the mismatch losses for both standard and half-cell modules in a hypothetical case where n strings are connected in a single MPP, each one with its respective shading pattern. The losses are analysed for different shading patterns and subject to an in-illumination irradiance range of 100-1000 W/m^2. A direct comparison between both technologies shows that the standard modules are subject to about 64% more losses than the half-cell modules, or in other words, about two-thirds.

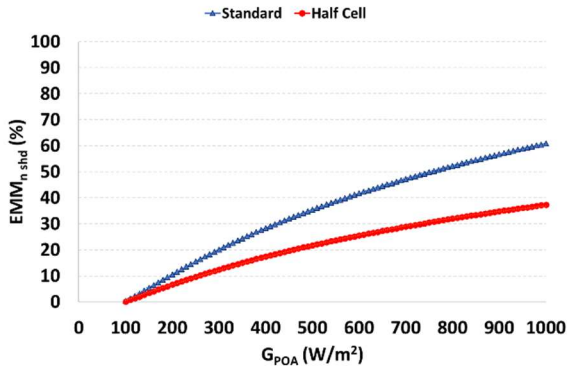

Figure 11: Mismatch losses vs in-illumination irradiance over the PV panels

A quadratic relationship allows the estimation of mismatch losses for these cases, for different irradiance levels.

$$MML_G(\%) = a\ G_{POA}^2 + b\ G_{POA} - c \quad (6)$$

where G_{POA} is the plane-of-array irradiance. The values of each coefficient are shown in Table III.

Table III: Coefficients for mismatch losses estimations from shading casts and in-illumination irradiance

	Half-cell	Standard cell
a	-2.10^{-5}	-4.10^{-5}
b	0.067	0.111
c	-5.82	-9.84

It is worth noting that these models were developed specifically for parallel connections. Its accuracy for series connections remains to be verified.

3.5 From substrings to an entire PV plant

These estimates are calculated for the entire PV plant and accumulated over a full year. Figure 12 shows the maximum energy produced by each string over the year for the same 70 MWp PV plant as shown in Fig. 7. The output of each string is then proportionally compared to the highest-producing string, as indicated by the colour scheme. In this instance, the maximum energy accumulated by a single string is 51.4 MWh.

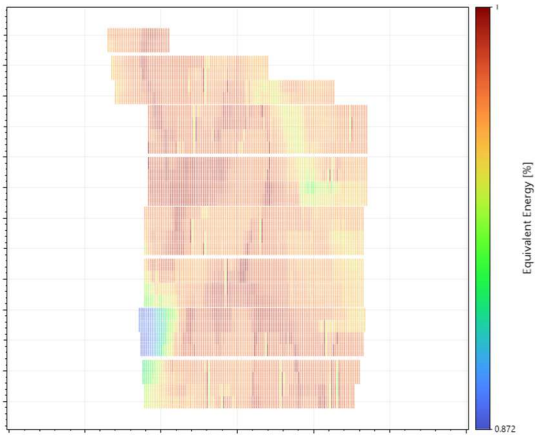

Figure 12: String maximum energy (accumulated) during a year for a 70 MW_p PV plant. The colours show the equivalent energy proportional to the string that produces the most energy

Fig. 13 depicts the maximum accumulated energy yielded by the inverters for the same PV plant and period. The total energy delivered in this case is 11.8 GWh.

10.4229/EUPVSEC2025/4DV.4.3
020432-005

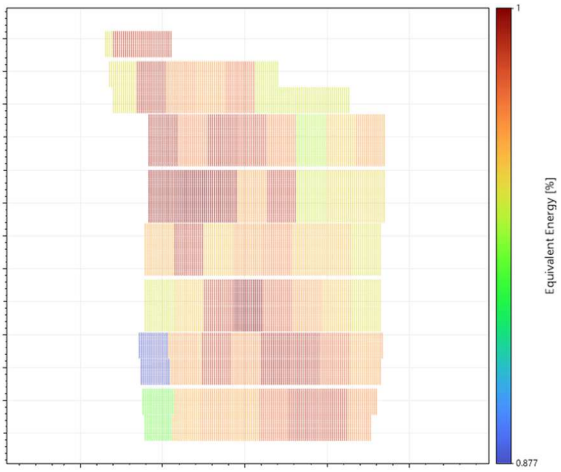

Figure 13: Inverter maximum energy (accumulated) during a year for a 70 MW_p PV plant. The colours show the equivalent energy proportional to the inverter that produces the most energy

For this PV plant, the combined Shading and Yield simulations ran about 43% faster than those based on I-V curves (40 min vs. 70 min). The yearly analysis considered roughly 85 transposition clusters and was carried out with a 15-minute time step. An interpolated simulation with the Sunveon model took 2.67 minutes in total, including per-string Shading Tables (0.32 min) and yield calculations (2.35 min). From this breakdown, it can be inferred that Shading calculations alone require 37.65 minutes. When isolating the yield component, the Sunveon model runs approximately 93% faster than full I-V curve simulations (2.35 min vs. 32.35 min). Although the extent of this computational gain depends on plant size, it remains highly significant even for smaller systems—for instance, around 75% faster for a 5 MW plant.

4 CONCLUSIONS

The challenge of accurately and efficiently estimating shading and mismatch losses in large-scale photovoltaic (PV) plants is a significant constraint for current production models. Conventional methods, which often rely on computationally expensive full I-V curve calculations or ray-tracing, can be slow. Conversely, simplified approaches may lead to substantial over- or underestimations of shading effects.

This study proposes the Sunveon Model, a novel and more efficient approach. It employs a hybrid transposition methodology, combining a 2D irradiance model with a 3D submodule-level shading model to accurately characterise incident irradiance on both standard and half-cell modules. A key advantage is its ability to estimate a string's Maximum Power Point (MPP) without requiring full I-V curve calculations, thus significantly reducing computational costs (between 75% and 93% for the yield calculation). The model also establishes a new method for quantifying mismatch losses using a 'Mixed Fill Factor,' allowing these losses to be calculated directly from a quadratic relationship.

The model's superior performance was validated against over 500,000 real I-V curves from five PV plants. The Sunveon Model consistently aligned more closely with this benchmark data compared to two industry-standard models, which were shown to systematically over or underestimate losses. Although errors for half-cell modules were slightly higher due to their more complex electrical topology, the model's performance remained highly precise, confirming its robustness.

A clear quadratic relationship was established between mismatch losses and both the percentage of cast shadow and the in-illumination irradiance. These equations allow for the direct estimation of losses. Notably, the analysis revealed that mismatch losses for standard cell modules are about two-thirds higher than for half-cell modules. It is important to note that these models were developed and validated specifically for parallel connections, with accuracy for series connections still to be verified.

In summary, the Sunveon Model offers a highly precise and robust tool for large-scale PV plant analysis, providing a valuable and computationally efficient alternative to existing methods by accurately modelling shading-induced and mismatch losses.

5 ACKNOWLEDGEMENTS

C.R. is partially supported by Torres Quevedo Grant No. PTQ2023-013183, funded by the Agencia Estatal de Investigación from the Spanish Ministry of Science. Most of the data used is available on the NREL web page, and the authors would like to thank them for it.

6 REFERENCES

[1] H. Rezk *et al.*, 'A novel statistical performance evaluation of most modern optimization-based global MPPT techniques for partially shaded PV system', *Renewable and Sustainable Energy Reviews*, vol. 115, Nov. 2019, doi: 10.1016/j.rser.2019.109372.

[2] O. Tsafarakis and W. G. J. H. M. van Sark, 'A density-based time-series data analysis methodology for shadow detection in rooftop photovoltaic systems', *Progress in Photovoltaics: Research and Applications*, vol. 31, no. 5, pp. 506–523, May 2023, doi: 10.1002/pip.3654.

[3] A. G. Olabi *et al.*, 'Artificial neural networks applications in partially shaded PV systems', *Thermal Science and Engineering Progress*, vol. 37, Jan. 2023, doi: 10.1016/j.tsep.2022.101612.

[4] R. Perez, P. Ineichen, R. Seals, J. Michalsky, and R. Stewart, 'Modeling daylight availability and irradiance components from direct and global irradiance', *Solar Energy*, vol. 44, no. 5, pp. 271–289, 1990, doi: 10.1016/0038-092X(90)90055-H.

[5] J. E. Hay, 'Calculation of monthly mean solar radiation for horizontal and inclined surfaces', *Solar Energy*, vol. 23, no. 4, pp. 301–307, 1979, doi: 10.1016/0038-092X(79)90123-3.

[6] M. A. Anoma, D. Jacob, B. C. Bourne, J. A. Scholl, D. M. Riley, and C. W. Hansen, 'View Factor Model and Validation for Bifacial PV and Diffuse Shade on Single-Axis Trackers', in *IEEE 44th Photovoltaic Specialists Conference (PVSC)*, Washington D.C., 2017, pp. 1549–1554. doi: 10.1109/pvsc.2017.8366704.

[7] D. Tschopp, A. R. Jensen, J. Dragsted, P. Ohnewein, and S. Furbo, 'Measurement and modeling of diffuse irradiance masking on tilted planes for solar engineering applications', *Solar Energy*, vol. 231, no. January, pp. 365–378, 2022, doi: 10.1016/j.solener.2021.10.083.

[8] A. Mermoud and T. Lejeune, 'Partial shading on PV arrays: by-pass diode benefits analysis', in *25th European Photovoltaic Solar Energy Conference*, Sep. 2010.

[9] C. Rossa, 'Energy losses in photovoltaic generators due to wind patterns', *Nature Communications Engineering*, vol. 2, no. 66, pp. 1–9, Sep. 2023, doi: 10.1038/s44172-023-00119-7.

[10] L. L. Bucciarelli, 'Power loss in photovoltaic arrays due to mismatch in cell characteristics', *Solar Energy*, vol. 23, no. 1, pp. 277–288, 1979.

[11] C. Rossa, F. Martínez-Moreno, and E. Lorenzo, 'Experimental observations in mismatch losses in monofacial and bifacial PV generators', *Progress in Photovoltaics: Research and Applications*, vol. 29, no. 12, pp. 1223–1235, Dec. 2021, doi: 10.1002/pip.3447.

[12] PVsyst, 'PVsyst shading calculation model - linear losses'. Accessed: Jul. 31, 2025. [Online]. Available: https://www.pvsyst.com/help-pvsyst7/shadings_model.htm

[13] M. Oliosi, B. Wittmer, and A. Mermoud, 'Analysis of Electrical Shading Effects in PV Systems', in *38th European PV Solar Energy Conference*, Sep. 2021, p. 2021.

[14] F. Martínez-Moreno, J. Muñoz, and E. Lorenzo, 'Experimental model to estimate shading losses on PV arrays', *Solar Energy Materials and Solar Cells*, vol. 94, no. 12, pp. 2298–2303, 2010, doi: 10.1016/j.solmat.2010.07.029.

[15] P. R. Satpathy and R. Sharma, 'Reliability and losses investigation of photovoltaic power generators during partial shading', *Energy Convers Manag*, vol. 223, Nov. 2020, doi: 10.1016/j.enconman.2020.113480.

[16] C. H. Rossa, E. Lorenzo, and F. Martínez-Moreno, 'Observations in PV module operation voltage distribution aling a PV array. An in-deep look on mismatch losses', in *35th European Photovoltaic Solar Energy Conference and Exhibition*, Brussels, 2018, pp. 2051–2055. doi: 10.4229/35thEUPVSEC20182018-6DV.1.38.

[17] R. Evans, M. Boreland, and M. A. Green, 'A holistic review of mismatch loss: From manufacturing decision making to losses in fielded arrays', *Solar Energy Materials and Solar Cells*, vol. 174, pp. 214–224, Jan. 2018, doi: 10.1016/J.SOLMAT.2017.08.041.

[18] C. Deline, S. Ayala Pelaez, S. MacAlpine, and C. Olalla, 'Estimating and parameterizing mismatch power loss in bifacial photovoltaic systems', *Progress in Photovoltaics: Research and Applications*, vol. 28, no. 7, pp. 691–703, Jul. 2020, doi: 10.1002/pip.3259.